Supplemental Discussion

We have made every effort to compare our simulations with the available NMR data (1,2). Our calculated S^2-values are consistent with experimental values, which report dynamics in the pico- to nano-second range, in describing the wt and the affects of the A53T and A30P mutations (Fig S3). Despite this, there are several areas where the observed dynamics deviate from those average values reported, though direct comparison is not trivial given the range of times over which these motions are averaged in the NMR experiment. Few published reports exist on calculating the S^2 parameter from simulation and comparing directly with experimental values. A recent attempt to match S^2 from simulations of the soluble protein lysozyme reported a root-mean squared error (RMSE) of 0.07 (3). This is only slightly better matching than our resulting RMSE of 0.1 for αS, a considerably more complicated system which contains large amplitude dynamics and is stabilized by interaction with an amorphous complex. Our S^2 data was calculated with a lower time resolution of 10 ps, and thus some of the fastest timescale dynamics are not reflected in that data set. Discrepancies in this calculation may be improved upon in future simulations by increasing this sampling rate, though the results also present an opportunity to improve the simulation analysis algorithms and potential energy functions. Given our relative success, we present our calculated S^2 values for the E46K mutant in anticipation of future experimental study.

The agreement between the simulations and the NMR experiments is poorest in residues up- and down-stream of the turn region (residues 38-44) which is not deeply bound, but rather sits in the micelle-water interface. This is in agreement with one study (4), but contradicts another (5). It has been speculated that the behavior of this region is dependent on the micelle size (6), something we did not address, though it is also possible that it is a product of the starting configurations we chose. In an effort to resolve this issue, we built and simulated a number of systems in which the turn region started immersed in the detergent, as has been done in the case of antimicrobial peptides (7,8). In none of these simulations of αS, however, did equilibration of the detergent lead to a structure that stabilized the turn-dynamics, nor did the turn region remain buried.

1. Ulmer, T. S., and Bax, A. (2005) *J Biol Chem* **280**, 43179-43187
2. Ulmer, T. S., Bax, A., Cole, N. B., and Nussbaum, R. L. (2005) *J Biol Chem* **280**, 9595-9603
3. Buck, M., Bouguet-Bonnet, S., Pastor, R. W., and MacKerell, A. D., Jr. (2006) *Biophys J* **90**, L36-38
4. Mihajlovic, M., and Lazaridis, T. (2008) *Proteins* **70**, 761-778
5. Bisaglia, M., Tessari, I., Pinato, L., Bellanda, M., Giraudo, S., Fasano, M., Bergantino, E., Bubacco, L., and Mammi, S. (2005) *Biochemistry* **44**, 329-339
6. Jao, C. C., Der-Sarkissian, A., Chen, J., and Langen, R. (2004) *Proc Natl Acad Sci U S A* **101**, 8331-8336
7. Khandelia, H., and Kaznessis, Y. N. (2007) *J Phys Chem B* **111**, 242-250
8. Langham, A. A., and Kaznessis, Y. N. (2006) *Molecular Simulation* **32**, 193-201

Supplemental Figures

Fig. S1. C^{α} RMSF for DOPS bound αS in CHARMM and GROMOS force fields. Though these simulations were run with different force fields and ensembles, the shapes of the curves are consistent, and of particular importance the magnitudes throughout the helical regions (where we have done our analysis) are highly consistent.

Fig. S2. C^{α} RMSD for wt, A53T, A30P, and E46K for micelle-bound helix-N (*A*) and helix-C (*B*). *C.* Comparison of C^{α} RMSD for micelle-bound wt and unbound wt. RMSD of C^{α} for wt, A53T, A30P, and E46K for bilayer-bound helix-N (*D*) and helix-C (*E*).

Fig. S3. NMR S^2 order parameter for micelle-bound wt helix-N (A), wt helix-C (B), A30P helix-N (C), A30P helix-C (D), A53T helix-N (E), A53T helix-C (F), E46K helix-N (G), E46K helix-C (H). Simulation results shown in pink, experimental data from Ulmer et. al. shown in blue.

Fig. S4. Percent helicity in wild-type and A30P mutant shows decrease in helical content up- and down-stream of proline substitution.

Fig. S5. Backbone torsion angles for residues 27 (*A*), 29 (*B*), and 30 (*C*) for micelle-bound wt and A30P. These positions show more subtle fluctuations as the region loses and regains helicity.

Figure S1

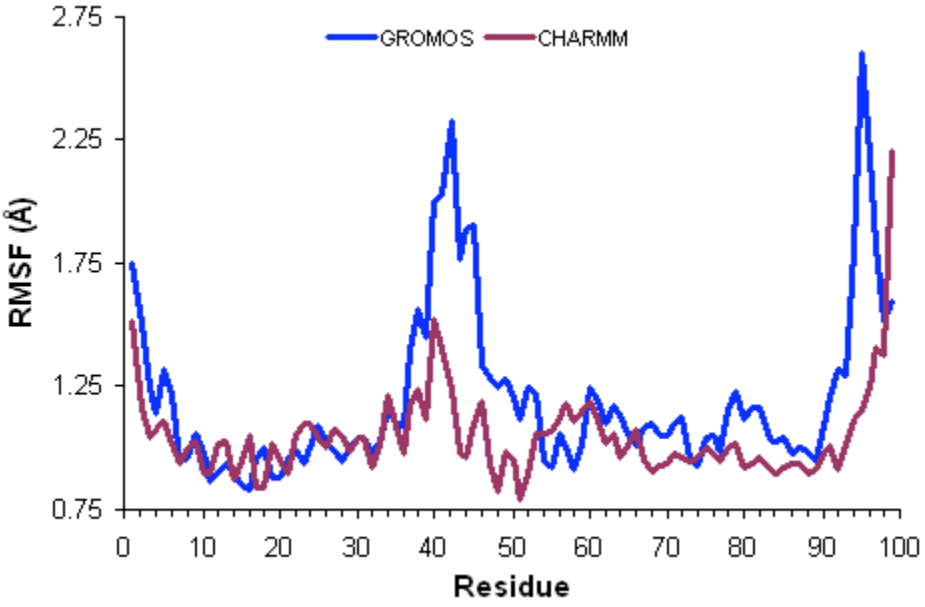
GROMOS
CHARMM
RMSF (Å)
2.75
2.25
1.75
1.25
0.75
0
10
20
30
40
50
60
70
80
90
100
Residue

Figure S2

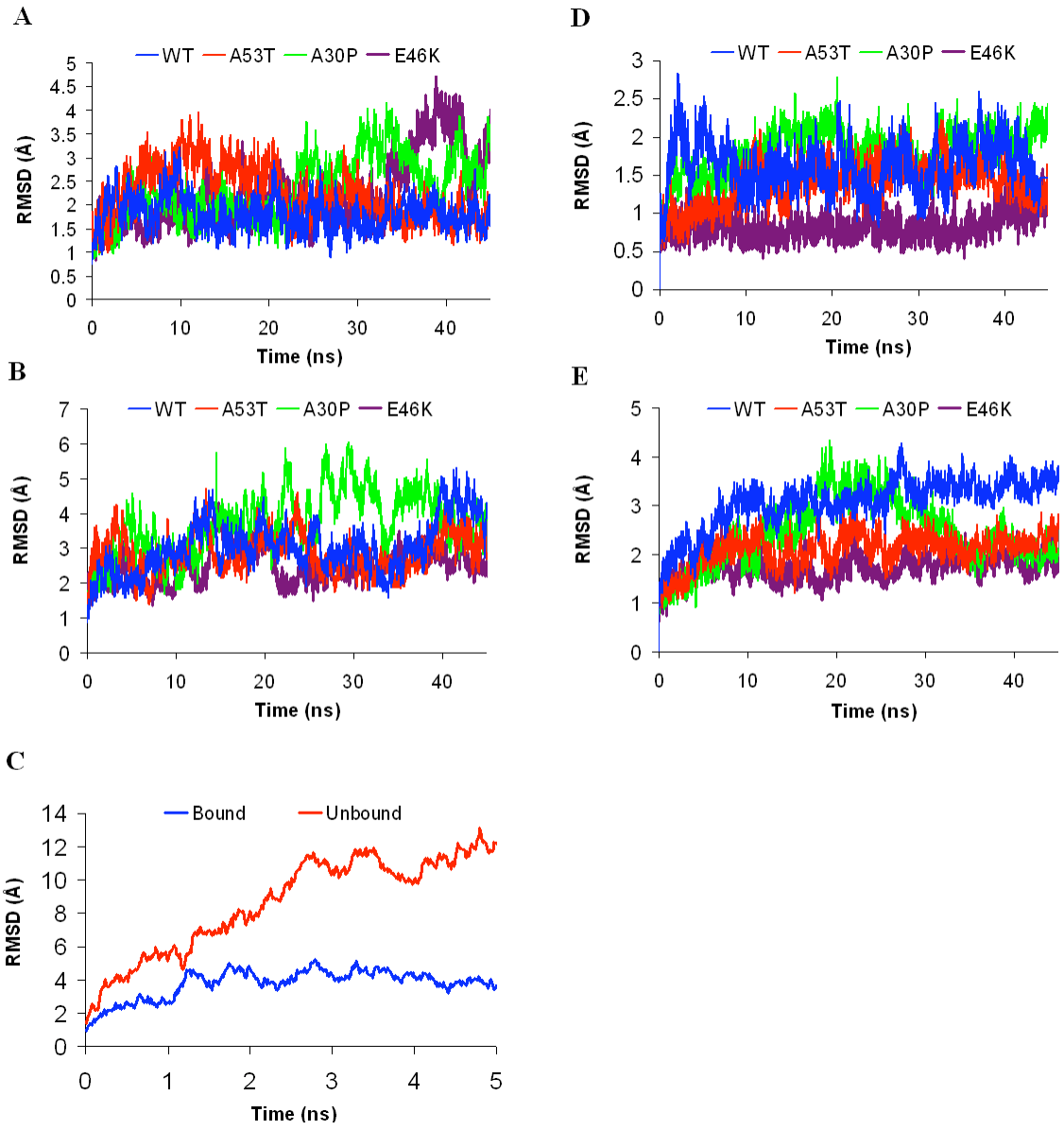

Figure S3

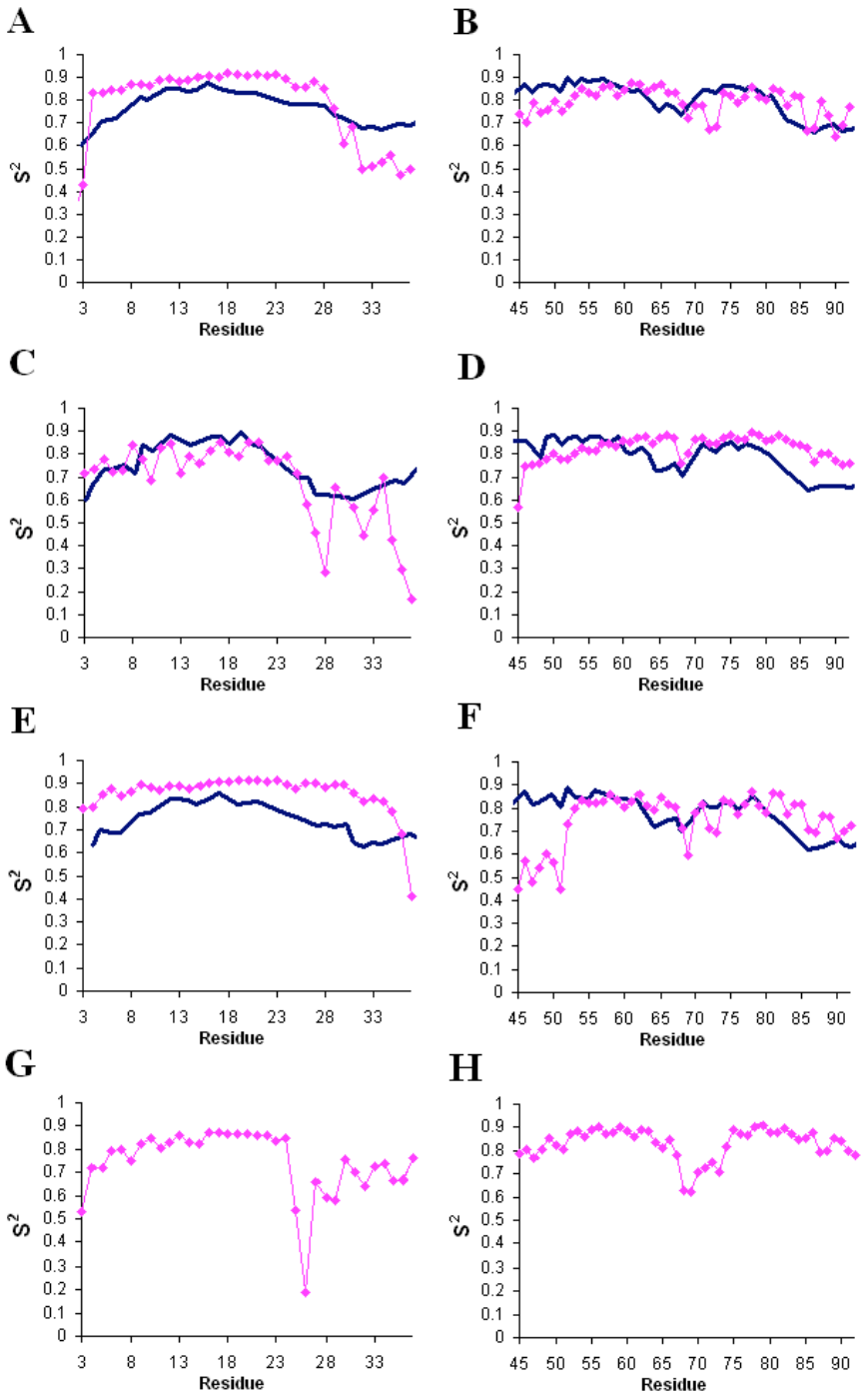
A
B
C
D
E
F
G
H
S2
Residue
3 8 13 18 23 28 33
45 50 55 60 65 70 75 80 85 90
0 0.1 0.2 0.3 0.4 0.5 0.6 0.7 0.8 0.9 1

Figure S4

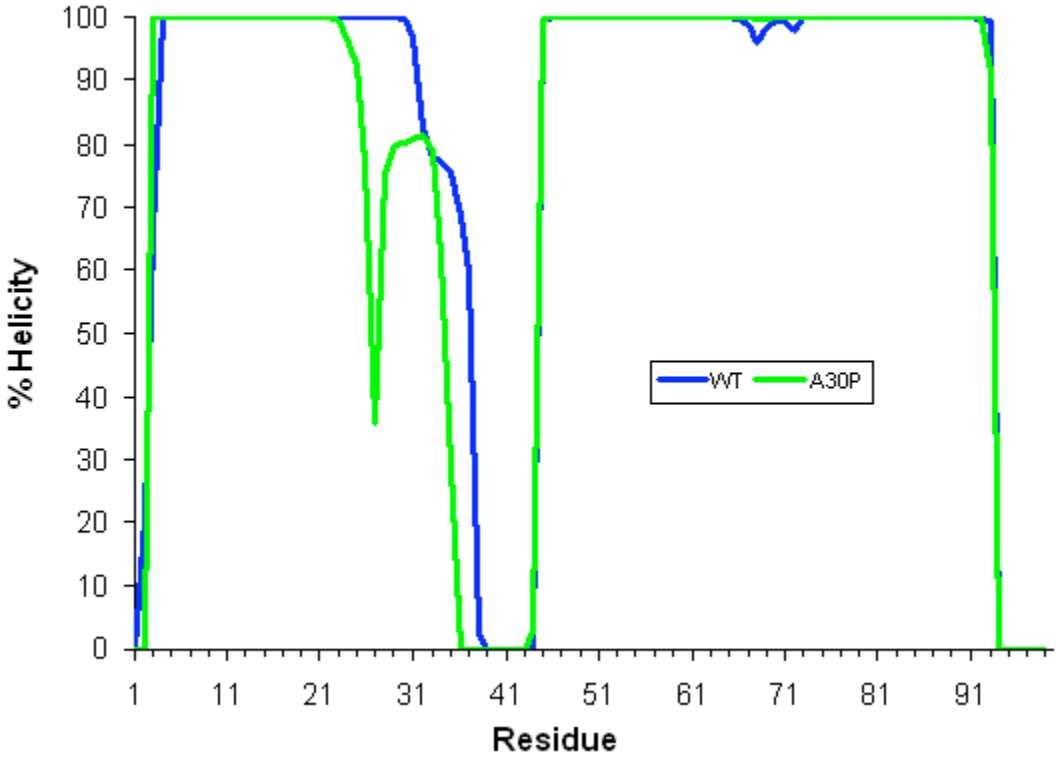
100
90
80
70
60
50
40
30
20
10
0
% Helicity
1
11
21
31
41
51
61
71
81
91
Residue
WT
A30P

Figure S5

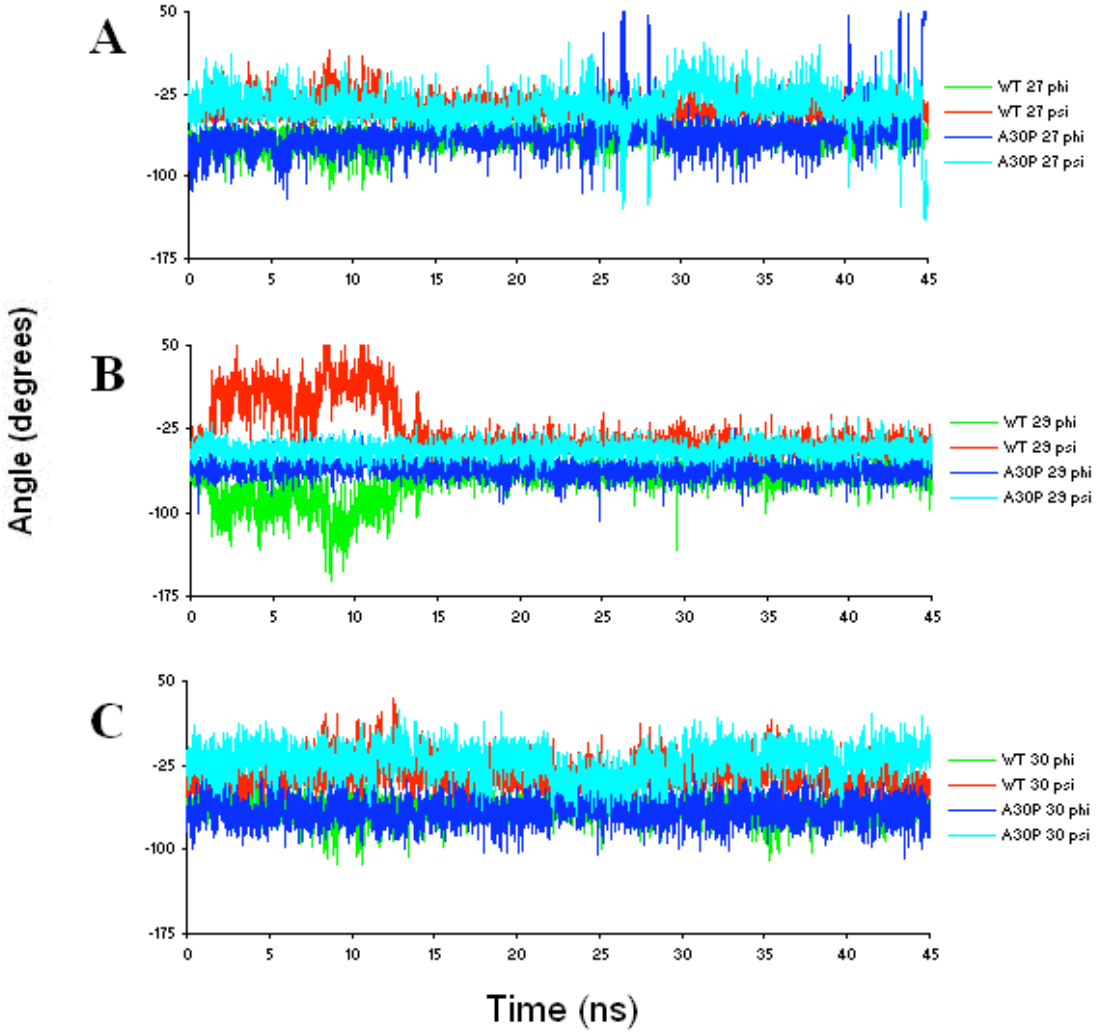
A
B
C
Angle (degrees)
Time (ns)
50
-25
-100
-175
0
5
10
15
20
25
30
35
40
45
WT 27 phi
WT 27 psi
A30P 27 phi
A30P 27 psi
WT 29 phi
WT 29 psi
A30P 29 phi
A30P 29 psi
WT 30 phi
WT 30 psi
A30P 30 phi
A30P 30 psi